Determination of the wavevector and temperature dependence of the `forbidden' mode in $Fe_{65}Ni_{35}$ Invar using inelastic neutron scattering



1996 J. Phys.: Condens. Matter 8 1527

(http://iopscience.iop.org/0953-8984/8/10/023)

J. Phys.: Condens. Matter **8** (1996) 1527–1538. Printed in the UK

# Determination of the wavevector and temperature dependence of the 'forbidden' mode in $Fe_{65}Ni_{35}$ Invar using inelastic neutron scattering

P J Brown†‡, B Roessli‡, J G Smith†, K-U Neumann† and K R A Ziebeck†

† Department of Physics, Loughborough University of Technology, Loughborough, Leicestershire LE11 3TU, UK

‡ Institut Laue–Langevin, BP 156, 38042 Grenoble Cédex 9, France

Received 19 October 1995, in final form 2 January 1996

**Abstract.** In previous polarized neutron inelastic scattering experiments on Fe–Ni alloys [1] a 'forbidden' mode was found at the Invar composition. This mode has the same dispersion as the transverse acoustic phonon, but was observed in longitudinal scans in which the momentum transfer was along the $(00\zeta)$ direction. The origin of this mode, which seems to be confined to the Invar composition, is not yet understood. This paper reports the results of an inelastic neutron scattering experiment using high-energy incident neutrons in which the mode has been found, and the wavevector dependence of its energy measured, in the first Brillouin zone. The intensity of the mode is greater in the first zone than in that centred on (200) and since the phonon cross section is minimized at small wavevectors it was concluded that the mechanism giving rise to the excitation is predominantly magnetic in origin. This conclusion receives support from the decrease in intensity of the mode with increasing temperature. On the basis of these results it is postulated that the 'forbidden' mode arises from a dynamic modulation of the magnetic moments associated with the compressive strain in the phonon excitations rather than from magnetovibrational scattering. These results together with the earlier polarized neutron measurements, indicating a frequency-dependent moment, are able to account for the anomalous thermal variation of the magnetization.

## 1. Introduction

The very low thermal expansion coefficient (the Invar effect) shown by certain magnetic alloys has been known of for a very long time, but even now is not completely understood. Nevertheless in all models of the Invar effect it is recognized that the relationship between magnetic moment and atomic volume or interatomic distance plays a crucial role and hence the interactions between the vibrational and magnetic degrees of freedom are of great importance. Consequently neutron scattering has been highly favoured amongst the many techniques used to investigate the Invar effect. Some years ago Ishikawa *et al* [2] postulated the existence of hidden excitations to account for the difference between the spin-wave stiffness constant determined from neutron scattering and that deduced from the temperature dependence of the magnetization. More recent neutron inelastic scattering measurements [1] have shown the existence of a 'forbidden' acoustic mode in the spectrum of excitations with wavevectors in the [001] directions. This excitation which has the same dispersion as the transverse acoustic (TA) mode has been seen in scans along reciprocal-space direction (100) with either (001) or $(1\bar{1}0)$ perpendicular to the scattering plane, although in neither case does

0953-8984/96/101527+12$19.50  

the polarization vector for the TA mode have a component parallel to the scattering vector $(0, 0, \zeta)$. The measurements were repeated under different experimental conditions, e.g. by changing the final wavevector, but the 'forbidden' mode was observed in all experiments. However, measurements carried out under identical experimental conditions on a Ni crystal and two NiFe crystals of different composition away from the Invar region failed to reveal the 'forbidden' mode. It was therefore concluded that the occurrence of this mode was intrinsic to the Invar composition.

Several models have been proposed to account for the Invar effect including latent antiferromagnetism [3] associated with fcc iron and atomic disorder [4]. However, since Invar properties are found in atomically ordered compounds compositional fluctuations can only be of secondary importance. Furthermore polarized neutron measurements on pure gamma iron [5] indicate that the paramagnetic state is characterized by strong ferromagnetic correlations with no evidence of any latent antiferromagnetism. It is now generally agreed that the Invar properties arise from large magnetovolume effects associated with the variation in amplitude of the local magnetic moment $\langle M^2(T)\rangle$. Indeed measurement of the polarization ratios of the one-phonon cross sections [1] have shown that the effective magnetic moments decrease as the phonon wavevector increases. The simplest mechanism which will produce a variation in the amplitude is Stoner excitations but this possibility has been eliminated on the basis of polarized neutron measurements [6]. Recent fixed-moment spin-polarized total energy band-structure calculations for the Invar alloy $Fe_{65}Ni_{35}$ [7] indicate the coexistence of almost degenerate states which are characterized by different magnetic moments and also by different volumes. Low-spin (LS) solutions are found with small atomic volume and high-spin (HS) solutions with large atomic volume. The coexistence of such HS and LS states can explain the absence of significant thermal expansion [8]. It has also been suggested [9] that the volume-coupled HS $\rightarrow$ LS transitions could be Ishikawa's 'hidden excitations'. More recently [10] it has been shown that distortions of a tetragonal or orthorhombic symmetry can also give rise to a HS$\rightarrow$LS transition in Invar. A model calculation has been reported which shows how slow lattice distortions can break the symmetry of the phonon modes and might give rise to the 'forbidden' mode [11]. It is, however, difficult to see how such a relatively small loss of symmetry alone can give rise to such a strong symmetry-breaking mode.

The properties of the band structure outlined above suggest an alternative origin for the 'forbidden' mode, since it can be expected that the HS $\rightarrow$ LS transition will couple to any of the phonon modes which effectively change the nearest-neighbour distances. In general in such a case the magnetic part of the inelastic one-phonon scattering cross-section will contain two terms, one due to the modulation of the displacement of the magnetic atoms and the second due to the modulation of their moments. The first term is the usual magneto-acoustic scattering whose intensity is proportional to $\boldsymbol{Q}^2\boldsymbol{\epsilon}\cdot\boldsymbol{\kappa}/(|\boldsymbol{\epsilon}||\boldsymbol{\kappa}|)$ where $\boldsymbol{Q}$ is the scattering vector, $\boldsymbol{\epsilon}$ the polarization vector and $\boldsymbol{\kappa}$ the wavevector of the phonon. The intensity of the second term depends on the magnitude of the moment modulation and this in turn on the nearest-neighbour distance, so it should be proportional to $[\boldsymbol{\epsilon}\cdot\boldsymbol{r}/(|\boldsymbol{\epsilon}||\boldsymbol{r}|)](1-\cos\boldsymbol{\kappa}\cdot\boldsymbol{r})$ where $\boldsymbol{r}$ is the vector joining nearest neighbours. For the TA [100] mode in the fcc structure $\boldsymbol{\epsilon}\cdot\boldsymbol{r}/(|\boldsymbol{\epsilon}||\boldsymbol{r}|)$ is $1/\sqrt{2}$ so scattering of this type is allowed. Not only does the magnetic modulation scattering have a different polarization factor from the magneto-acoustic scattering but it also has no $\boldsymbol{Q}^2$-dependence, it should therefore be possible to observe such scattering in the first Brillouin zone even though $\boldsymbol{Q}^2$ has such a small value that the magneto-acoustic scattering should be very weak.

In this paper the results of an inelastic neutron scattering study of the 'forbidden' mode in $Fe_{65}Ni_{35}$ using high-energy incident neutrons are reported. The use of high incident

energies enables scans to be carried out in the first Brillouin zone and so can test whether the 'forbidden' mode arises in whole or in part from the magnetic modulation described above.

## 2. Experimental procedure

The conditions under which neutron scattering can take place are determined by the following energy and momentum conservation rules:

$$\Delta E = \frac{\hbar^2}{2m}\left(k_i^2 - k_f^2\right) \tag{1}$$

$$\hbar \boldsymbol{Q} = \hbar \boldsymbol{k}_i - \hbar \boldsymbol{k}_f \tag{2}$$

where $\Delta E$ is the energy transfer and $\boldsymbol{k}_i$ and $\boldsymbol{k}_f$ are the incident and final neutron wavevectors. Equation (2) can be rewritten in terms of the scattering angle $\phi$ as

$$Q^2 = k_i^2 + k_f^2 - 2|\boldsymbol{k}_i||\boldsymbol{k}_f|\cos(\phi). \tag{3}$$

When carrying out triple-axis spectroscopy it is usual to fix the magnitude of either $\boldsymbol{k}_i$ or $\boldsymbol{k}_f$ and vary the other in order to provide the energy transfers required.

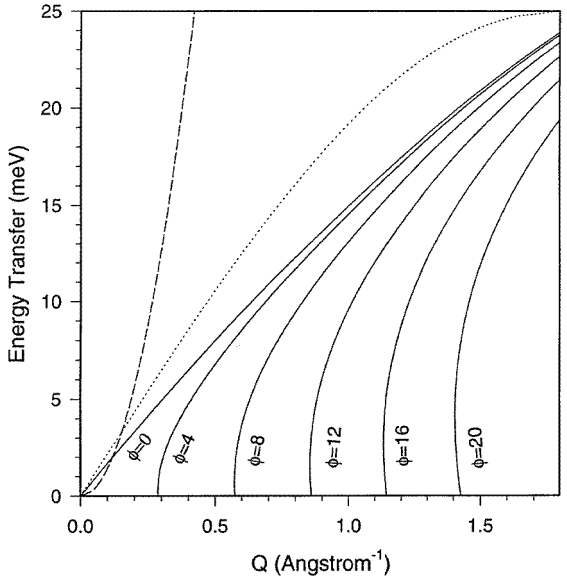


**Figure 1.** The range of energy and momentum transfers available at different scattering angles $\phi$ between 0° and 20° using an incident neutron energy of 35 meV ($k_i = 4.1$ Å$^{-1}$). This incident energy can be provided by a triple axis on a thermal source but is towards the upper end of the energy range generally used. Shown also in the figure is the dispersion of the spin wave (dashed line) and forbidden mode (dotted line). Under these experimental conditions it is impossible to observe the forbidden mode and the spin wave is only accessible at very small energy transfers using a scattering angle close to zero, which would give rise to problems such as increased background.

As the energy transfer is increased the momentum transfer increases also, and therefore in order to close the scattering triangle, equation (3), $\phi$ must also increase. In order to carry out scans at finite energy transfers in the first Brillouin zone it is necessary to increase

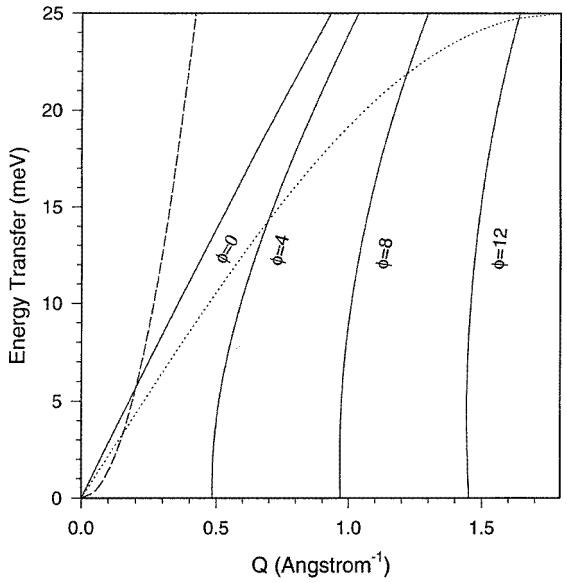


**Figure 2.** The range of energy and momentum transfers available at different scattering angles $\phi$ between 0° and 20° using an incident neutron energy of 100 meV ($k_i = 6.96$ Å$^{-1}$) which is readily available on a hot-source triple axis. From this figure it may be seen that the spin wave can again only be investigated in the limit of small scattering angle but that the forbidden mode is now fully accessible. However, other practical difficulties such as background and scan width effectively restrict measurements to above 15 meV for this particular experimental configuration.

either $\boldsymbol{k}_i$ or $\boldsymbol{k}_f$. The range of energy and momentum transfer required is determined by the dispersion of the 'forbidden' mode. If equation (1) is substituted into (3) the range of momentum–energy space accessible for given incident neutron wavevector can be determined. The results are shown in figures 1 and 2 for incident neutron energies 35 meV ($\boldsymbol{k}_i = 4.1$ Å$^{-1}$) and 100 meV ($\boldsymbol{k}_i = 6.96$ Å$^{-1}$) respectively. The dispersion curves for the magnon ($D = 143$ meV Å$^2$), the LA phonon and the 'forbidden' mode 24 meV Å$^{-1}$ along the [100] direction are superposed. From these figures it is clear that the 'forbidden' mode is not observable in the first zone for any scattering angle if the incident energy is only 35 meV which was that used in previous experiments. Increasing the incident energy to 100 meV enables the 'forbidden' mode to be observed for energy transfers above 15 meV at a scattering angle of 4°. Experimentally the minimum accessible scattering angle, which is determined by the proximity of the straight-through beam, was found to be 2.5°. Thus by careful selection of the incident energy it is possible to investigate the dispersion of the 'forbidden' mode in the first Brillouin zone for energy transfers greater than 15 meV.

The experiment was carried out on the same single crystal of $Fe_{65}Ni_{35}$ as used in previous neutron experiments [1]. The crystal which was in the form of a cube of side 12 mm was mounted with the [1$\bar{1}$0] axis vertical inside a variable-temperature cryostat on the triple-axis spectrometer IN1 at the ILL in Grenoble. IN1 is located on the hot source which provides the high-energy incident neutrons needed for the experiment. The exterior tail of the cryostat was increased to a diameter of 1.0 m in order to reduce the background scattering at small scattering angles. As in previous experiments the temperature was initially set to 100 K well below the Curie temperature of 550 K, but later scans were also carried out at room temperature and above the Curie temperature at 570 K.

The spectrometer was set up with a vertically focusing Cu(200) monochromator and the scattered beam was also analysed using a Cu(200) crystal. Preliminary scans were carried out around (002) using collimation of 30′, 40′, 40′ and 40′ with respect to the outgoing beam, but in order to work in the first zone close to the straight-through position it was necessary to tighten the collimation in front of and behind the specimen to 20′. One point in the scans was measured until a fixed number of counts were registered by the monitor placed in the beam between the monochromator and the sample, so the time per point was dependent on the incident energy and was of the order of five minutes. The spectrometer was operated throughout in the constant-$\boldsymbol{k}_f$ mode with $\boldsymbol{k}_f$ set to 5.7 Å$^{-1}$ for the majority of scans although for some it was necessary to increase $\boldsymbol{k}_f$ to 6.6 Å$^{-1}$. As a further check that the 'forbidden' mode was intrinsic to the material some scans were repeated with the curvature of the monochromator set to zero, i.e. flat, to improve the vertical resolution and, as expected, there was no change in the observed excitations.

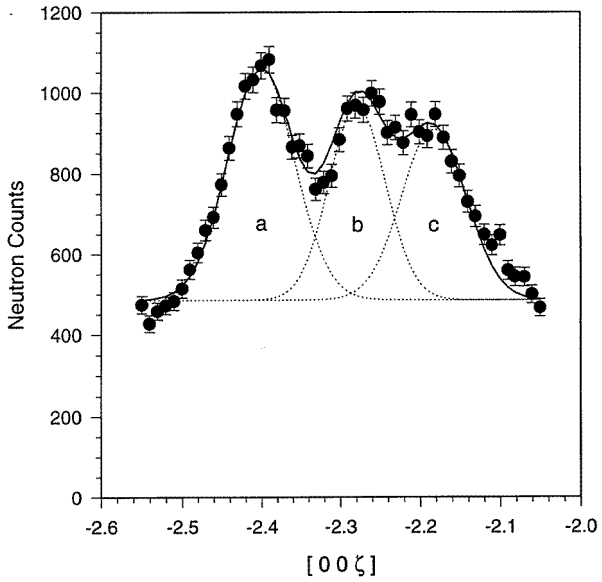


**Figure 3.** A longitudinal scan along the $(0\,0-\zeta)$ direction in the zone centred on $(0\,0-2)$ using $k_f = 5.7$ Å$^{-1}$ and an energy transfer of 15 meV. The scan reveals three inelastic features confirming the results of earlier polarized neutron measurements [1]. The peaks which are labelled a, b and c represent the forbidden mode, longitudinal phonon and spin wave respectively, all of which are propagating in the $(0\,0-\zeta)$ direction at a temperature of 100 K. From the figure it may be seen that the forbidden mode is the dominant feature.

## 3. Results

Initial measurements were carried out in the zone centred on (002) in order to compare the results with those obtained previously under different experimental conditions on IN20. Thus a series of constant-energy scans with $\boldsymbol{Q} = (0, 0, 2 \pm \zeta)$ were undertaken for energy transfers between 15 and 20 meV using collimation of 30′, 40′, 40′ and 40′. The results of one of these scans, which were all consistent with the previous data, are shown in figure 3. From this figure it may be seen that there are three distinct excitations centred

on $\zeta = 0.4$, 0.27 and 0.17 corresponding to the 'forbidden' mode, the longitudinal phonon and the magnon. The wavevector dependence of the energies of these modes was given in figure 2. As mentioned earlier the dispersion of the 'forbidden' mode is the same as that of the degenerate transverse acoustic mode in the [001] direction although with the scattering geometry used the cross section for that excitation is zero. Nevertheless it is clear from figure 3 that this mode is the dominant feature of the spectrum and, as extensive measurements have shown previously, is an intrinsic property of the material.

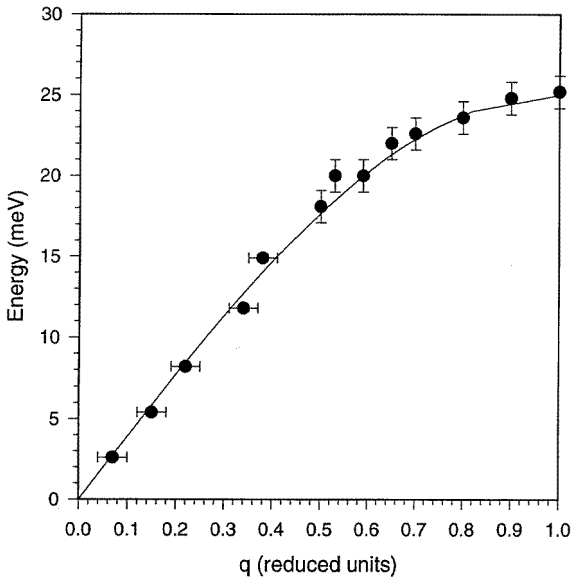


**Figure 4.** The dispersion of the forbidden mode determined using longitudinal scans in which the scattering vector was parallel to the $(0\,0\,-\zeta)$ direction. The dispersion curve was measured at 100 K in the zone centred on (002).

Having reconfirmed the presence of the 'forbidden' mode in the zone based on (002), the study was then continued in the first Brillouin zone. An initial longitudinal scan along the (001) direction with an energy transfer of 18 meV showed a strong excitation centred at a reduced lattice vector $q = 0.48$ in agreement with the measurements made in the third zone. Moreover the intensity scattered by the mode was significantly greater than in the zone centred on (002). Unfortunately due to the restrictions placed on the kinematic range by the conservation rules it was not possible to observe either the longitudinal phonon or the magnon for comparison. With the tighter collimation mentioned above the wavevector dependence of the energy of the mode was measured out to the zone boundary; the results are shown in figure 4.

Having established the existence of the 'forbidden' mode and determined its dispersion in the first zone the measurements were repeated after warming to 300 K. These measurements which were confined to constant-$\boldsymbol{q}$ scans from $q = 0.7$ out to the zone boundary $q = 1.0$ indicated that the intensity of the mode decreased as the temperature was raised. It was therefore decided to heat the sample above the Curie temperature and again repeat the measurements in the first zone. For this it was necessary to remount the crystal in a cryofurnace which allowed temperature variation between 150 and 580 K. The Curie temperature was verified by monitoring the temperature of the (002) Bragg peak as the

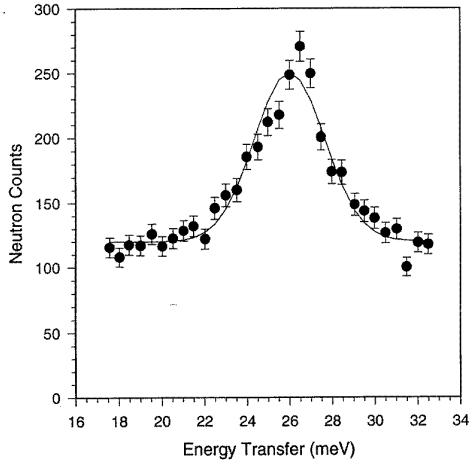


**Figure 5.** A constant-$Q$ scan in the first Brillouin zone at the (001) zone boundary showing the forbidden mode at a temperature of 100 K.

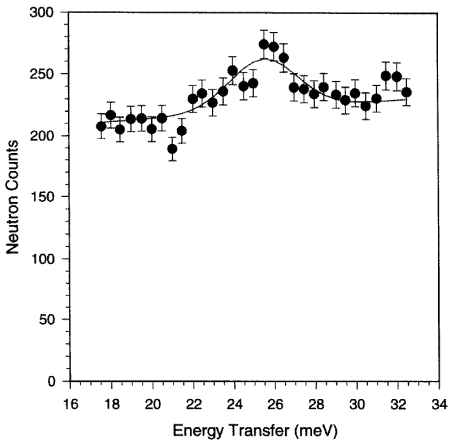


**Figure 6.** A constant-$Q$ scan in the first Brillouin zone at the (001) zone boundary showing the forbidden mode at a temperature of 550 K.

temperature was raised. The high-temperature scans showed that excitations with the same energies as those observed at lower temperatures persist above the Curie temperature but that their intensity is substantially diminished (figure 5). In contrast the intensity of the TA [001] phonon measured at the zone boundary (221) significantly increased with temperature between 300 and 550 K.

## 4. Magnetovibrational scattering with spin fluctuations driven by interatomic strain

Squires [12] (p 138) gives the cross-section for spin-only scattering by atoms with localized moments in a Bravais crystal like $Fe_{65}Ni_{35}$ as

$$\frac{\mathrm{d}^2\sigma}{\mathrm{d}\Omega\ \mathrm{d}E'} = (\gamma_n r_0)^2 \frac{k'}{k} \sum_{\alpha\beta} (\delta_{\alpha\beta} - \hat{\boldsymbol{Q}}_\alpha \cdot \hat{\boldsymbol{Q}}_\beta) \sum_{l'} \sum_{l} F^*(\boldsymbol{Q}) F(\boldsymbol{Q}) \times \sum_{\lambda\lambda'} p_\lambda \langle\lambda'|\exp(-\mathrm{i}\boldsymbol{Q}\cdot\boldsymbol{R}_{l'})\boldsymbol{S}_{l'}^{\alpha}|\lambda\rangle\langle\lambda'|\exp(-\mathrm{i}\boldsymbol{Q}\cdot\boldsymbol{R}_{l})\boldsymbol{S}_{l}^{\beta}|\lambda\rangle. \tag{4}$$

Here $\gamma_n$ is the neutron magnetic moment in nuclear magnetons and $r_0$ is the classical electron radius; $\boldsymbol{Q}$ is the scattering vector, $F(\boldsymbol{Q})$ is the magnetic structure factor, $\boldsymbol{R}_l$ is the position of the atom at lattice site $\boldsymbol{l}$ and $\boldsymbol{S}_l^{\beta}$ the $\beta$-component of its spin. $E$ and $\boldsymbol{k}$ are the energy and wavevector of the incident neutron, and $\lambda$ represents the initial state of the scattering system and $p_\lambda$ its probability. The primed symbols are the final-state values. The last line of equation (4) can be written [12] as

$$\frac{1}{2\pi\hbar}\int_{-\infty}^{\infty} \langle\exp(-\mathrm{i}\boldsymbol{Q}\cdot\boldsymbol{R}_{l'}(0))\boldsymbol{S}_{l'}^{\alpha}(0)\exp(-\mathrm{i}\boldsymbol{Q}\cdot\boldsymbol{R}_{l}(t))\boldsymbol{S}_{l}^{\beta}(t)\rangle \exp(-\mathrm{i}\omega t)\ \mathrm{d}t \tag{5}$$

where

$$\boldsymbol{S}_l^{\beta}(t) = \exp(\mathrm{i}Ht/\hbar)\boldsymbol{S}_l^{\beta}\exp(-\mathrm{i}Ht/\hbar).$$

The angle brackets in equation (5) indicate the thermal average of the enclosed operator at the temperature of the system. If there is no correlation of either the magnitudes

or the directions of the magnetic moments of the atoms with their displacements $\boldsymbol{u} = \boldsymbol{R}_l - \boldsymbol{l}$ then the thermal average of equation (5) can be factorized into the product of an average depending only on the atomic displacements and one depending only on magnetic fluctuations. The product may be expanded to give four terms corresponding to magnetic elastic scattering, magnetovibrational scattering, inelastic scattering in just the spin system and finally inelastic scattering in both the phonon and spin systems. The term of interest here is the magnetovibrational scattering which is elastic in the spin system and inelastic in the phonon system. It gives scattering with the same dependence $\boldsymbol{q}$, $\boldsymbol{Q}$ and $\omega$ as phonon scattering by the atomic nuclei except that the $\sigma_{coh}/4\pi$ which occurs in the nuclear phonon cross-section is replaced by $\frac{1}{4}(\gamma_n r_0)^2 F^2(\boldsymbol{Q})(1-\hat{Q}_z^2)\langle \boldsymbol{S}^z\rangle^2$ in the magnetovibrational cross-section. Both cross-sections are proportional to

$$\frac{(\boldsymbol{\epsilon}\cdot\boldsymbol{Q})^2}{\omega} \rightarrow \left[\frac{(\boldsymbol{\epsilon}\cdot\boldsymbol{Q})^2}{\boldsymbol{v}\cdot\boldsymbol{q}}\right]_{lim(q\rightarrow 0)} \propto \boldsymbol{Q} \tag{6}$$

where $\boldsymbol{\epsilon}$ is the polarization of the phonon, $\boldsymbol{v}$ the phonon velocity and $\boldsymbol{q}$ the reduced wavevector. From this it may be seen that for $\boldsymbol{Q} \parallel [001]$ the cross-section for the TA [001] phonon is zero, but it is with exactly this geometry that the 'forbidden' mode, which has the $\boldsymbol{q}\omega$-dependence of the [001] TA phonon, is observed.

The origin of the 'forbidden' mode may be sought in the breakdown of the approximation which allows factorization of the thermal average in equation (5). This will no longer be justified if, as is suggested by band-structure calculations [3], there are volume-coupled transitions between HS and LS states. Suppose for simplicity that the effect of the transitions from HS to LS states can be approximated by a linear dependence of the magnitude of the magnetic moment on the strain in the interatomic bonds, and furthermore that such transitions take place on a time scale much faster than the phonon frequencies. With these assumptions the spins can be renormalized to

$$\boldsymbol{S}_i = \boldsymbol{S}_{i0}\left(1 - x\sum_j \varepsilon_{ij}\left[\Delta R_i - \Delta R_j\right]\right) \tag{7}$$

where $\varepsilon$ is the strain between nearest-neighbour atoms, $x$ a constant of proportionality and $\Delta R_i$ is the deviation of the atom at lattice site $i$ from its equilibrium position. Assuming that the renormalization is small the thermal average of equation (5) may now be factorized as

$$\left\langle \exp(-\mathrm{i}\boldsymbol{Q}\cdot\boldsymbol{R}_{l'}(0))\exp\left(-x\sum_{d'} u_{l'}\varepsilon_{l'd'}u_{d'}\right)\exp(-\mathrm{i}\boldsymbol{Q}\cdot\boldsymbol{R}_l)\exp\left(-x\sum_d u_l\varepsilon_{ld}u_d\right)\right\rangle \times\left\langle \boldsymbol{S}_{l'}^{\alpha}(0)\cdot\boldsymbol{S}_l^{\beta}(t)\right\rangle \tag{8}$$

and this average may be developed to give four terms similar to those enumerated above. The thermal average which determines the magnetovibrational scattering is now

$$\begin{aligned}&\left\langle \exp(-\mathrm{i}\boldsymbol{Q}\cdot\boldsymbol{R}_{l'}(0))\exp\left(-x\sum_{d'} u_{l'}\varepsilon_{l'd'}\right)\exp(-\mathrm{i}\boldsymbol{Q}\cdot\boldsymbol{R}_l(t))\exp\left(-x\sum_d u_l\varepsilon_{ld}u_d\right)\right\rangle \\ &\qquad\times\langle \boldsymbol{S}_{l'}^{\alpha}(0)\cdot\boldsymbol{S}_l^{\beta}(\infty)\rangle \\ &\quad= \left\langle \exp(-\mathrm{i}\boldsymbol{Q}\cdot\boldsymbol{R}_{l'}(0))\exp\left(-x\sum_{d'} u_{l'}\varepsilon_{l'd'}(0)u_{d'}\right)\exp(-\mathrm{i}\boldsymbol{Q}\cdot\boldsymbol{R}_l(t))\right. \\ &\qquad\left.\times\exp\left(-x\sum_d u_l\varepsilon_{ld}(t)u_d\right)\right\rangle(1-\hat{\kappa}_z^2)\langle S^z\rangle^2.\end{aligned} \tag{9}$$

The strain due to thermal vibrations can be written in terms of the displacements $\boldsymbol{u}$ and the vector separation $\boldsymbol{r}$ of nearest neighbours to give

$$\frac{x}{|r|^2}\hat{\boldsymbol{r}}\cdot\frac{\partial\tilde{\boldsymbol{u}}}{\partial\boldsymbol{l}} = \mathrm{i}\xi\hat{\boldsymbol{r}}\cdot q\left(\frac{\hbar}{2MN}\right)^{1/2}\sum_s\frac{\boldsymbol{e}_s}{\sqrt{\omega}}\left\{a_s\exp(\mathrm{i}\boldsymbol{q}\cdot\boldsymbol{l}) + a_s^\dagger\exp(-\mathrm{i}\boldsymbol{q}\cdot\boldsymbol{l})\right\} \tag{10}$$

with $\xi = x/|r|^2$. $a$ and $a^\dagger$ are the annihilation and creation operators for the phonons, and the sum is over all the occupied phonon states $s$. Following [12] (p 29) the thermal average can be developed in terms of the product of the exponentials of two operators $U$ and $V$ with

$$U = -\mathrm{i}\left(\boldsymbol{Q}\cdot\boldsymbol{u}_0(0) + \xi\left(\frac{\mathrm{d}\boldsymbol{u}}{\mathrm{d}\boldsymbol{l}}\right)_0(0)\right) = -\mathrm{i}\sum_s\left(a_s(g_s+\gamma_s) + a_s^\dagger(g_s+\gamma_s)\right) \tag{11}$$

$$V = \mathrm{i}\left(\boldsymbol{Q}\cdot\boldsymbol{u}_l(t) + \xi\left(\frac{\mathrm{d}\boldsymbol{u}}{\mathrm{d}\boldsymbol{l}}\right)_l(t)\right) = \mathrm{i}\sum_s\left(a_s(h_s+\eta_s) + a_s^\dagger(h_s+\eta_s)\right) \tag{12}$$

$$g_s = \left(\frac{\hbar}{2MN}\right)^{1/2}\frac{\boldsymbol{Q}\cdot\boldsymbol{e}_s}{\sqrt{\omega}_s} \qquad \gamma_s = \left(\frac{\hbar}{2MN}\right)^{1/2}\frac{\xi q\boldsymbol{r}\cdot\boldsymbol{e}_s}{\sqrt{\omega}_s}$$

$$h_s = \left(\frac{\hbar}{2MN}\right)^{1/2}\frac{\boldsymbol{Q}\cdot\boldsymbol{e}_s}{\sqrt{\omega}_s}\exp\left(\mathrm{i}(\boldsymbol{q}\cdot\boldsymbol{l} - \omega_s t)\right)$$

$$\eta_s = \left(\frac{\hbar}{2MN}\right)^{1/2}\frac{\xi q\boldsymbol{r}\cdot\boldsymbol{e}_s}{\sqrt{\omega}_s}\exp\left(\mathrm{i}(\boldsymbol{q}\cdot\boldsymbol{l} - \omega_s t)\right).$$

The magnetovibrational cross-section can then be written as

$$\left(\frac{\mathrm{d}^2\sigma}{\mathrm{d}\Omega\ \mathrm{d}E'}\right)_{MV} = (\gamma_n r_0)^2\frac{k'}{k}\frac{N}{2\pi\hbar}\exp\langle U^2\rangle\sum_l\exp(\mathrm{i}\boldsymbol{Q}\cdot\boldsymbol{l})\int_{-\infty}^{\infty}\exp\langle UV\rangle\exp(-\mathrm{i}\omega t)\ \mathrm{d}t. \tag{13}$$

The Debye–Waller term is

$$\exp\langle U^2\rangle = \exp\left[\left(\frac{\hbar}{2MN}\sum_s\frac{1}{\omega_s}\left((\boldsymbol{Q}+\xi q\hat{\boldsymbol{r}})\cdot\boldsymbol{e}_s\right)^2\right)\langle 2n+1\rangle\right] = \exp(-2W'). \tag{14}$$

The one-phonon cross-section is obtained from the term in $\langle UV\rangle$ in the expansion of $\exp\langle UV\rangle$:

$$\exp\langle\lambda|UV|\lambda\rangle = \sum_{ss'}\langle\lambda|\left(a_s(g_s+\gamma_s) + a_s^\dagger(g_s+\gamma_s)\right)\left(a_{s'}(h_{s'}+\eta_{s'}) + a_{s'}^\dagger(h_{s'}^*+\eta_{s'}^*)\right)|\lambda\rangle \tag{15}$$

giving

$$\begin{aligned}\langle UV\rangle &= \sum_s\left((g_s+\gamma_s)(h_s^*+\eta_s^*)\langle n_s+1\rangle + (g_s+\gamma_s)(h_s+\eta_s)\langle n\rangle\right)\\ &= \left(\frac{\hbar}{2MN}\right)\sum_s\frac{\left((\boldsymbol{Q}+\xi q\hat{\boldsymbol{r}})\cdot\boldsymbol{e}_s\right)^2}{\omega_s}\left(\exp(-\mathrm{i}(\boldsymbol{q}\cdot\boldsymbol{l}-\omega_s t))\langle n_s+1\rangle\right.\\ &\quad\left.+\exp(\mathrm{i}(\boldsymbol{q}\cdot\boldsymbol{l}-\omega_s t))\langle n\rangle\right).\end{aligned} \tag{16}$$

The cross-section for magnetovibrational scattering by one-phonon creation is thus

$$\begin{aligned}\left(\frac{\mathrm{d}^2\sigma}{\mathrm{d}\Omega\ \mathrm{d}E'}\right)_{MV+1} &= (\gamma_n r_0)^2\frac{k'}{k}\frac{(2\pi)^3}{2Mv_0}\exp(-2W')\sum_s\sum_\tau\frac{\left((\boldsymbol{Q}+\xi q\hat{\boldsymbol{r}})\cdot\boldsymbol{e}_s\right)^2}{\omega_s}\langle n_s+1\rangle\\ &\quad\times\delta(E-E'-\omega_s)\,\delta(\boldsymbol{Q}+\boldsymbol{q}-\boldsymbol{\tau})\end{aligned} \tag{17}$$

where $\boldsymbol{\tau}$ is a reciprocal-lattice vector. The factor $\left((\boldsymbol{Q}+\xi q\hat{\boldsymbol{r}})\cdot\boldsymbol{e}_s\right)^2$ appearing in equation (17) is to be compared with the simple $(\boldsymbol{e}_s\cdot\boldsymbol{Q})^2$ appearing in the unmodified expression for magnetovibrational scattering. The modified expression is finite even when $\boldsymbol{e}_s\cdot\boldsymbol{Q}=0$ and its magnitude then is proportional to $q^2$ rather than to the $Q^2$ characteristic of pure phonon scattering, so its intensity in the first Brillouin zone is enhanced over that in higher zones by the $Q$-dependence of the magnetic form factor. The above considerations show that magnetic fluctuations driven by changes in interatomic spacing can give rise to scattering which has the characteristics found for the 'forbidden' mode.

The relative magnitudes of the magnetic and nuclear contributions to the phonon intensity depend on two additional factors: the form factor $f(\boldsymbol{Q})$ and the relative magnitudes of the Debye–Waller terms $\exp(-2W')$ and $\exp(-2W)$ where the Debye–Waller factors are responsible for the polarization dependence of the phonon intensity and its variation in $\boldsymbol{q}$.

## 5. Discussion

Although the 'forbidden' mode has the same dispersion as the TA [001] phonon, experiment has shown that its neutron scattering cross-section is not due to phase shifts due to the atomic displacements introduced by this phonon since these give a $\boldsymbol{Q}^2$-dependence of intensity and moreover have no component parallel to the scattering vector in the geometry of the experiment. Previous experiments have shown that this is intrinsic to the material but peculiar to the Invar composition $Fe_{65}Ni_{35}$. In this experiment the 'forbidden' mode has been observed in the first zone where the phonon cross-section is small. In fact the 'forbidden' mode intensity increases by more than a factor of two on going from the Brillouin zone centred on (002) to the first Brillouin zone, e.g. from the zone boundary at (003) to that at (001). Furthermore, the one-phonon cross section decreases significantly as the wavevector decreases. The scattering vector $\boldsymbol{Q}$ for the (001) and (003) zone-boundary positions is 1.77 $\text{Å}^{-1}$ and 5.3 $\text{Å}^{-1}$ respectively, which would produce a ninefold decrease in the phonon intensity. The magnetic form factor increases by approximately 3.5 in going from (003) to (001) giving rise to an increase by a factor of 12 in the magnetic intensity. Therefore it would appear that the presence of the 'forbidden' mode is in part due to magnetic interactions, the strength of which would increase with the magnetic form factor at small $\boldsymbol{Q}$. Support for this conjecture is provided by the decrease in the intensity of the mode as the specimen temperature is raised. However, the mode has only decreased in intensity by ~75% on heating to just above the Curie temperature. This implies that either the mechanism giving rise to the 'forbidden' mode is not entirely magnetic in origin or else that the strong spatial correlations known to be important in Invar are able to maintain the interaction above $T_c$. It should be noted that earlier polarized neutron measurements gave rise to a polarization ratio for the 'forbidden' mode. Such a ratio would not be possible if the mode were purely magnetic in origin. The intensity of the phonon just above the magnetic transition at 550 K is determined by the product of two factors. The Bose factor

$$n(\boldsymbol{q})=\frac{1}{\exp(\hbar\omega(\boldsymbol{q})/k_BT)-1}+1 \tag{18}$$

gives rise to an increase of ~2.5 with respect to that at 100 K, while the loss of magnetic order produces a decrease of intensity as determined by $\left(1-\frac{2}{3}\gamma^2\right)$ where $\gamma=F_M/F_N$, i.e. the ratio of the magnetic and nuclear structure factors. As a result the expected increase in intensity would therefore be $\sim 0.8\times 2.5$ which gives a factor of 2 whereas experimentally a decrease by at least a factor of 4 is found.

The thermal variation of the magnetization, particularly at low temperatures, has long been an unresolved problem. Ishikawa *et al* [2] noted that spin waves only account for half of the decrease in the magnetization of $Fe_{65}Ni_{35}$ and proposed the existence of a hidden excitation to account for this discrepancy. To date the existence of a hidden mode has not been established and the present results suggest that an additional mode is unnecessary. The discrepancy between the spin-wave and magnetization measurements only occurs at the Invar composition, there being good agreement in $Fe_{50}Ni_{50}$. Similarly the 'forbidden' mode is intrinsic to the Invar composition and is absent in $Fe_{50}Ni_{50}$. The 'forbidden' mode is not an additional excitation but arises from a coupling of the lattice and magnetic degrees of freedom, and therefore when accounting for the thermal variation of the magnetization it is necessary to consider not only the magnetic but also the lattice fluctuations and the coupling between them. Neutron scattering and ultrasonic measurements [13] have revealed a softening of phonon frequencies below $T_c$. The softening is confined to TA modes with wavevectors extending out into the middle of the zone. Previous polarized neutron measurements [1] of the polarization ratios of the acoustic phonon modes have revealed that the local moment decreases by approximately a factor of 2 with increasing phonon frequency from the Brillouin centre. Assuming that the thermal population of the coupled modes is given by the Bose factor, then by making use of the polarized neutron results indicating a frequency-dependent reduction of the moment, the thermal variation of the magnetization may be modelled assuming

$$M(\boldsymbol{q}) = M\left(1 - \frac{q^{\nu}}{q_c^{\nu}}\right) \tag{19}$$

where $\nu$ determines the rate at which the moment decreases and $\boldsymbol{q}_c$ is the cut-off wavevector. Thus the thermal variation of the magnetic moment is obtained by averaging over the phonon density of states with the normalization determined by a fixed moment system, namely

$$M(T) = \left(\int \frac{M_0(1 - q^{\nu}/q_c^{\nu})q^2}{\exp(\hbar\omega(q)/k_BT) - 1}\ \mathrm{d}q\right)\left[\int \frac{M_0 q^2}{\exp(\hbar\omega(q)/k_BT) - 1}\ \mathrm{d}q\right]^{-1} \tag{20}$$

$$M(T) \propto T^{\nu}. \tag{21}$$

According to the analysis of the magnetization data by Ishikawa *et al* [2] and Yamada and Nakai [14] the discrepancy between the observed thermal decrease of the magnetization and that predicted by the experimental spin-wave dispersion suggests that $\nu$ should take a value between 1.5 and 2. This analysis depends on the value of the spin-wave stiffness constant used in the analysis which is obtained from neutron scattering measurements at finite $\boldsymbol{q}$. Since the magnetization is a $Q = 0$ measurement this can lead to an unsatisfactory analysis of the magnetization measurements particularly if the spin-wave dispersion is steep. Such difficulties were encountered in nickel, but since $Fe_{65}Ni_{35}$ has a much smaller spin-wave stiffness constant this may be less problematic. The possible values of $\nu$ suggested by the analysis are consistent with the earlier polarized neutron measurements [1] indicating a frequency-dependent moment.

Model calculations by Kim and co-workers [15] have shown that electron–phonon coupling in itinerant magnets can be important and the thermal population of phonons is as effective as spin waves in accounting for the thermal variation of the magnetization. The effectiveness of the phonons in accounting for the decrease in magnetization depends upon the details of the band structure at the Fermi level. Band-structure calculations indicate that the Fermi level is located just above the majority $t_{2g}$ and in between the $t_{2g}$ and $e_g$ minority peaks in the DOS. A decrease in the nearest-neighbour distance broadens the $t_{2g}$

minority sub-band, causing repopulation between the minority $t_{2g}$ and $e_g$ sub-bands. For a critical nearest-neighbour distance, the change in occupancy of the $t_{2g}$ minority orbitals is large enough to move the majority atomic levels with $t_{2g}$ character and to move the $t_{2g}$ majority peak from just below $E_F$ to partly above. The magnetic moment is sensitively dependent on the interatomic spacing.

Both of these models given by Kim and Lipinski suggest that the HS→LS transition is associated with the critical interatomic distance. Our simple model on the other hand assumes a linear sinusoidal dependence which can be taken as a first term in the Fourier expansion of the moment versus distance dependence of the models involving the critical distance.

## 6. Conclusions

A model has been put forward here which relates the neutron scattering by the 'forbidden' mode to the coupling between magnetic and lattice degrees of freedom. This model requires that the mean magnetic moment be a function of the occupation of the phonon modes. This requirement accords with previous spin-polarized measurements of the polarization dependence of the phonon intensities, which have shown a frequency-dependent moment [1]. Clearly the coupling between magnetic moments and phonons must be taken into account when calculating the temperature dependence of the magnetization and could account for the discrepancy between experimental observation and the predictions based on the spin-wave stiffness constant as determined by neutron scattering [2].

## Acknowledgments

The authors wish to thank P Palleau for technical support, and JGS and KRAZ thank the EPSRC for financial support. Helpful comments from A S Alexandrov, H Capellmann, S Lipinski and J H Samson are gratefully acknowledged.

## References

[1] Brown P J, Jassim I K, Neumann K-U and Ziebeck K R A 1989 *Physica* B **161** 9
[2] Ishikawa Y, Onodera S and Tajima K 1979 *J. Magn. Magn. Mater.* **10** 183
[3] Kondorsky E I and Sedov V L 1960 *J. Appl. Phys.* **31** 331S
[4] Menshikov A Z 1979 *J. Magn. Magn. Mater.* **10** 205
[5] Brown P J, Capellmann H, Deportes J, Givord D and Ziebeck K R A 1983 *J. Magn. Magn. Mater.* **30** 335
[6] Ishikawa Y, Noda Y, Ziebeck K R A and Givord D 1986 *Solid State Commun.* **57** 531
[7] Mohn P, Schwartz K and Wagner D 1991 *Phys. Rev.* B **43** 3318
[8] Moroni E G and Jarlborg T 1989 *Physica* B **161** 115
[9] Wassermann E F 1990 *Ferromagnetic Materials* vol 5, ed K H Buschow and E P Wohlfarth (Amsterdam: North-Holland)
[10] Lipinski S 1995 *J. Magn. Magn. Mater.* **140–144** 233
[11] Lipinski S, Neumann K-U and Ziebeck K R A 1995 *J. Phys.: Condens. Matter* **6** 9773
[12] Squires G L 1978 *Introduction to the Theory of Thermal Neutron Scattering* (Cambridge: Cambridge University Press)
[13] Endoh Y 1979 *J. Magn. Magn. Mater.* **10** 177
[14] Yamada O and Nakai I 1981 *J. Phys. Soc. Japan* **50** 823
[15] Kim D J 1983 *Physica* B **119** 30
Yoshida I and Kim D J 1995 *J. Magn. Magn. Mater.* **140–144** 217